86 GHz VLBI Survey of Ultracompact Radio Emission in Active Galactic Nuclei

Nair, Dhanya G.[1]; Lobanov, Andrei P.[1,2]; Krichbaum, Thomas P[1].; Ros, Eduardo[1].; Zensus, Anton J.[1]

[1]Max-Planck-Institut für Radioastronomie, Auf dem Hügel 69,53121,Bonn,Germany
[2]Institut für Experimentalphysik,Universitat Hamburg,Luruper Chausse 149,22761,Hamburg,Germany

E-mail : dhanya@mpifrbonn.mpg.de; alobanov@mpifrbonn.mpg.de; tkrichbaum@mpifr-bonn.mpg.de; eros@mpifr-bonn.mpg.de ; azensus@mpifr-bonn.mpg.de

Abstract

Very Long Baseline Interferometry (VLBI) Observations at 86 GHz reach a resolution of about 50 microarcseconds and sample the scales as small as 10^3- 10^4 Schwartzchild radii of the central black hole in Active Galactic Nuclei (AGN), and uncover the jet regions where accelaration and collimation of the relativistic flow takes place. Synchrotron radiation becomes optically thin at millimetre wavelengths ; making it possible to look deeper into the core and inner jets of AGN which is invisible at cm and longer wavelengths due to self absorption or free-free absorption by the torus. We present here results from a large global VLBI survey of 168 ultracompact radio sources at 86 GHz conducted in 2010 - 2011. All the sources were detected and imaged ; increasing by a factor of ~ 2 the total number of AGN imaged with VLBI at 86 GHz. We use gaussian modelfitting to represent the structure of the observed sources. The modelfitting yields estimates of the brightness temperature (T_b) of the VLBI bright core (base) of the jet and inner jet components of AGN, taking into account the resolution limits of the data at 3mm. We also compare the brightness temperature of the VLBI cores from this 86 GHz survey with similar estimates from the MOJAVE VLBI surveys at 15 GHz. We also compare the brightness temperatures obtained from the model fits with estimates of the brightness temperature limits made directly from the visibility data. For objects with sufficient structural detail detected, we investigate the effect of adiabatic energy losses on the evolution of brightness temperature along the jet.

Key words: general - galaxies: active - galaxies : jets - quasars : general - radio continuum : galaxies - surveys : galaxies - brightness temperature.

1. Introduction

Many galaxies host a very luminous nuclei,which is brighter than the remaining galaxy light. They are called Active Galactic Nuclei (AGN). They are active in the entire electro magnetic spectrum with radiation coming from radio to gamma ray wave bands, with much of the energy of non thermal origin. AGNs are believed to host a supermassive black hole of mass of order ~ (10^6 - 10^9) M_o , which power the relativistic jet of plasma to large distances even Mpc. Very Long Baseline Interferometry (VLBI) observations at 86 GHz (wavelength of 3 mm) of such radio sources gives a very high angular resolution of 40 – 100μas and zoom into their most compact central region; to linear scales as small as 10^3 - 10^4 Schwarzschild radii. Thus the 3 mm VLBI makes it possible to image directly the subparsec scale regions which is very close to the central black hole; which is invisible at cm and longer wavelengths due to self absorption or free-free absorption by the torus surrounding the core and uncovers the structure of the jet regions where acceleration and collimation of the jet flow takes place.

To date, five 86 GHz VLBI surveys have been conducted (Beasley1997, Lonsdale1998, Rantakyro1998, Lobanov 2000,Lee 2008) with the total number of objects imaged reaching just over a hundred. According to Homan 2006 and Cohen 2007,the high-resolution studies of complete (or nearly complete) samples of compact jets yield a wealth of information about the intrinsic properties of compact extragalactic flows. This survey established hybrid maps of 168 unique radio sources increasing the total number of sources ever imaged with 86 GHz by a factor of 2.

In this paper, we present results from a large global vlbi survey of compact radio sources begun in October 2010. The main goal of the survey was to extend the existing survey at 86 GHz to faint sources and to develop a comprehensive sample of ultra compact radio sources that are imaged at 86 GHz and to increase the VLBI imaging database ; study the morphology and the distribution of brightness temperatures and to investigate collimation and acceleration of relativistic flows and to probe physical conditions in the vicinity of supermassive black holes.The sample selected is complete down to ~ 0.5 Jy at 86 GHz for declination ≥ -20 degree.The survey data attained a baseline sensitivity of 0.1 Jy and the image sensitivity of 5 mJy/beam. A total of 168 compact radio sources have been observed in this survey. Out of the 168 sources observed, all sources are detected and imaged. The sample consists of quasars, galaxies, blazars and unidentified sources. Flux densities and sizes of all core and jet components have been measured using gaussian model fitting. From these measurements the brightness temperature have been estimated taking into account the limits on the resolution of the data.

Measuring brightness temperature in a statistically viable sample enables investigations of the physical conditions in this region. The distribution of the observed brightness temperatures T_b,derived at 86 GHz can be combined with the T_b distributions measured at lower frequencies (Kovalev 2005). This can help constraining the bulk Lorentz factor and the intrinsic brightness temperature,T_o of the jet plasma, using different types of population models of relativistic jets like in Lobanov 2000.

In Sect.2,we describe the source selection,observations and the data processing. Some of the images obtained from the observations

are presented in Sect.3.1. In Sect.3.2.1, we present the distribution of brightness temperatures measured in the observed sample of sources and in Sect.3.2.2, the evolution of observed brightness temperature along the jet in the sub parsec scales is checked for the theoretical predictions of brightness temperature for the adiabatic expansion in a relativistic plasma (Marsher 1995) for few sources. In Sect.3.3, we discuss a different approach for obtaining the T_b directly from the visibility data as discussed by Lobanov 2015 and discuss the corelation of T_b measurements by gaussian method approach and visibility based estimates in this large sample of sources. In Section 3.4, we combine the T_b measurements from this 86 GHz survey with MOJAVE sample at 15 GHz (Kovalev 2005). Throughout this paper, we used the positive definition of spectral index,α (S proportional to υ^{α}) and assume a Hubble constant H_o= 100 $kms^{-1}Mpc^{-1}$.

Table 1. *VLBI surveys at 86 GHz*

Survey	N_{ant}	B_{rec}	ΔS	ΔIm	D_{img}	N_{obs}	N_{det}	N_{img}
Beasley et al. (1997)	3	112	~ 0.5	...	...	51	12	...
Lonsdale et al. (1998)	2-5	112/224	~ 0.7	...	...	79	14	...
Rantakyro et al.(1998)	6-9	128	~ 0.5	~ 30	70	68	16	12
Lobanov et al. (2000)	3-5	224	~ 0.4	~ 20	100	28	26	14
Lee et.al (2008)	12	256	~ 0.3	~ 10	200	127	121	109
This survey	**13-14**	**512**	**~ 0.1**	**~ 5**	**>440**	**168**	**168**	**168**

Columns: 1 – survey; 2 - number of participating antennas; 3 - recording bit rate [Mbps]; 4-average baseline sensitivity [Jy]; 5 - average image sensitivity [mJy/beam]; 6 - typical dynamic range of images; 7 - number of objects observed; 8 - number of objects detected; 9 - number of objects imaged.

2. Methods

2.1 Source selection

The sources list contains 168 objects selected from the MOJAVE complete sample (Kovalev et.al 2005) and 22 GHz VERA Galactic plane survey (Petrov et.al 2007) using the follwing criteria: a) corelated flux density ≥ 0.5 Jy on long baselines (≥400 Mλ); b) compactness ≥ 0.4 ; c) declination $\delta \geq -20^0$.

The target list (complete down to ~ 0.5 Jy level at 86 GHz) is selected from the 15 GHz VLBA survey database (Kovalev et.al 2005). This database includes all objects from the 15 GHz VLBA monitoring programmes. We use this database to select a complete flux density limited sample of objects that satisfies the following selection criteria: a) the sources selected are in the statistically complete MOJAVE sample (Lister 2005), allowing us to perform statistically significant analysis of the 86 GHz VLBI data; b) additional sources selected have the 15-GHz correlated flux density at the longest VLBA baselines (400 – 450 Mλ), $S_c > 500$ mJy and the compactness at longest spacings $S_c/S_{VLBA} > 0.4$. There is a total of 175 sources satisfying these criteria. A similar approach was applied to select objects for the Lee et al.(2008) survey that has yielded a nearly 100% detection rate. The selection criteria applied optimize the chances for a source to be detected at long baselines at 86 GHz.

2.2 Observations

The observations have been made over the total of 6 days (144 hours),scheduled within three separate Global Millimetre VLBI Array(GMVA) sessions. Up to 14 telescopes in USA and Europe – Efflesberg,Onsala, Pico Velata,Plateau de Bure,Yebes, Metasähovi and seven VLBA stations took part in the observation.The observations were made with 5 scans per hour, each of 300 seconds in duration. Gaps of 5 -10 minutes were introduced between the scans for antenna pointing (at Efflesberg and Pico Velata, this is an essential requirement for ensuring the accuracy of amplitude calibration of the survey data) and phasing of the Plateau de Bure interferometer. This observing scheme yielded the total of 720 scans divided between 168 observing targets, ensuring that each object was observed with 4-5 scans distributed over a wide range of hour angles.

The observations were performed at a sampling rate of 512 Mbit/sec and with a 2 bit sampling (128 MHz bandwidth). The baseline sensitivities for a 20 second fringe fitting are ~ 0.05 Jy on the PB-PV baseline, ~ 0.1Jy on the EB-PV baseline, ~ 0.2 Jy on the baselines between EB/PV and other antennas, and ~ 0.4 Jy on the VLBA baselines. With such baseline sensitivities, we acheived a point source sensitivity of ~ 5 mJy/beam, sufficient to obtain images of the survey sources.

Table 2. *Log of Survey Observations*

Epoch	$N_{sources}$	Bit rate ($Mbits^{-1}$)	Bandwidth	Frequency channels	Sampling (bits)	Telescopes
Oct 2010	72	512	128	32	2	8 VLBA+(EB,ON,Mh,PdB,PV)
May 2011	46	512	128	64	2	8 VLBA+(EB,On,PdB,PV,Mh)
Oct 2011	60	512	128	32	2	8 VLBA+(EB,On,PdB,PV,Mh,Ys)

2.3 Data Processing and calibration

The data were co related from the GMVA correlating facility in Max-Planck-Institut für Radioastronomie in Bonn. The data was loaded into AIPS (Astronomical Image Processing System). Even after applying the co relator model and possible corrections during correlation, there is still residual phase errors between the IFs. There can be gradient of phase in frequency that is the gradient within each IF (single band delay) and the gradient between IFs (multiband delay). This happens due to the unavoidable correlator models at each station that is errors in geometrical time delay at each station. This is because for 3mm, eventhough there is a radio window which allows the signal to reach earth, they are severly affected by the atmosphere. The inaccurate earth geometry,errors in the position of sources and antennas used ,errors in the clock epoch etc also affects the phases. The phase as well as the amplitude of the signal varies as a result of this and in 3mm VLBI observations the phases can vary so rapidly of the order of (10s –30 s). Since the phase as well as amplitude remains coherent for such a short time, it is important to look scan by scan to check whether fringe is detected or not. The phase varies not only as a function of frequency but also in time. This time dependent phase rates, is equivalent to the residual fringe rate. Fringes were searched with the AIPS task FRING to remove the frequency dependent as well as time dependent phase errors and line up the phases in all the IFs.

Once the global fring was done, the SNRs for all the sources were seperately inspected and strong sources which give relatively very high SNR were determined. While interpolating the solutions from the global fring , the fringe solutions from those strong sources were interpolated to nearby weak sources.

The amplitude calibration was done using the measured values of antenna gain and system temperature and the weather information from each station during the observation was used to apply the opacity corrections to the amplitude. From the phase and amplitude calibrated data, the images were made using hybrid mapping (Cornwell and Fomalont 1999) in DIFMAP software(Shepherd 1994). A detailed description on the phase and amplitude calibration and imaging will be given in Nair.D.G.,*PhDthesis,in prep.*

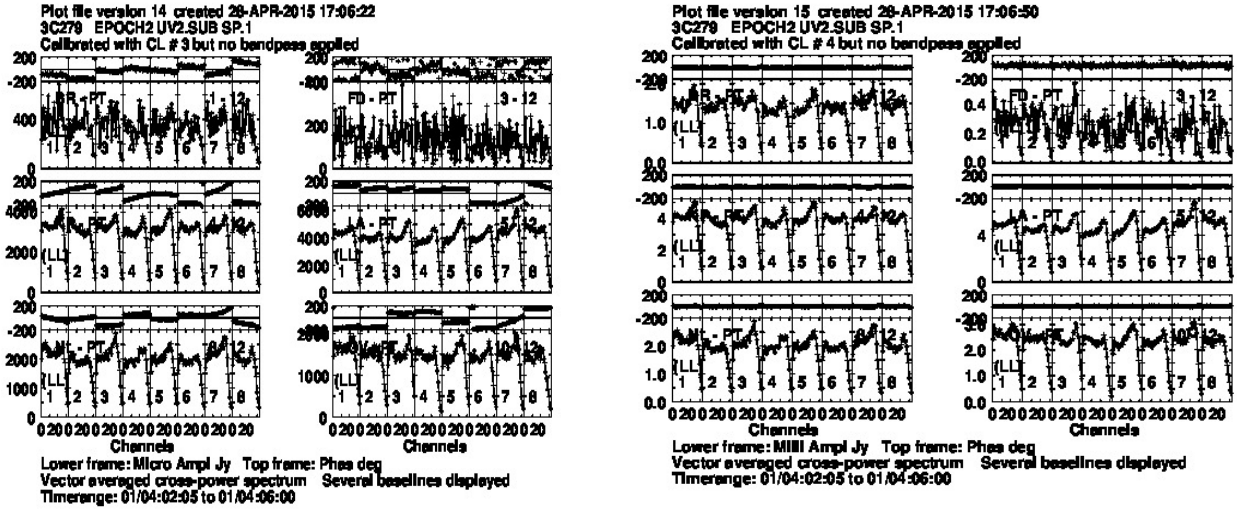

Fig.1 *Amplitudes and phases of VLBA baseline visibilities before (left panel) and after (right panel) fringe fitting and amplitude calibration for the source 3C279.*

3. Results and discussion

3.1 *3mm maps*

We model the visibility data for each source with a single or multi component gaussian model and check the agreement factor between the model and observed visibility amplitude(Lobanov 2000). The technique of model fitting(Lobanov 1996) is very useful to analyse poorly calibrated data and data with poor uv coverage and this method of modelfitting was applied to derive the source brightness distribution and to paramaterize the physical quantitites like size of the core and jet components,the position of jet components w.r.t core,uncertainities in such measurements etc from the images.

We have detected and made hybrid maps of 168 unique sources in this survey. There was a 100% detection rate and could image all the sources for which the data has sufficient uv coverage and closure phases. We have imaged all the 168 radio sources, increasing the database of sources imaged ever at 86 GHz by a factor of 2 . The morphology of most of the par sec- scale jets were revealed. For really weak sources with poor uv coverage we could image only the core which is close to the supermassive black hole and for other sources the sub parsec scale jet structure was also revealed.To illustrate our results, we present the images of two weak target radio sources J0700+1709 and J1130+3815 and two calibrator sources 3C345 and 0716+714.

a. J0700+1709

The source is an unidentified source. In the image in the Fig.2, we identify one feature in the jet extending along P.A 167.471 degree.The peak flux density is 0.234Jy/beam,with a beam size of 0.323x0.037 mas and the lowest contour is at 7 mJy. The brightness temperature of the core component is 1.928×10^{11} K.

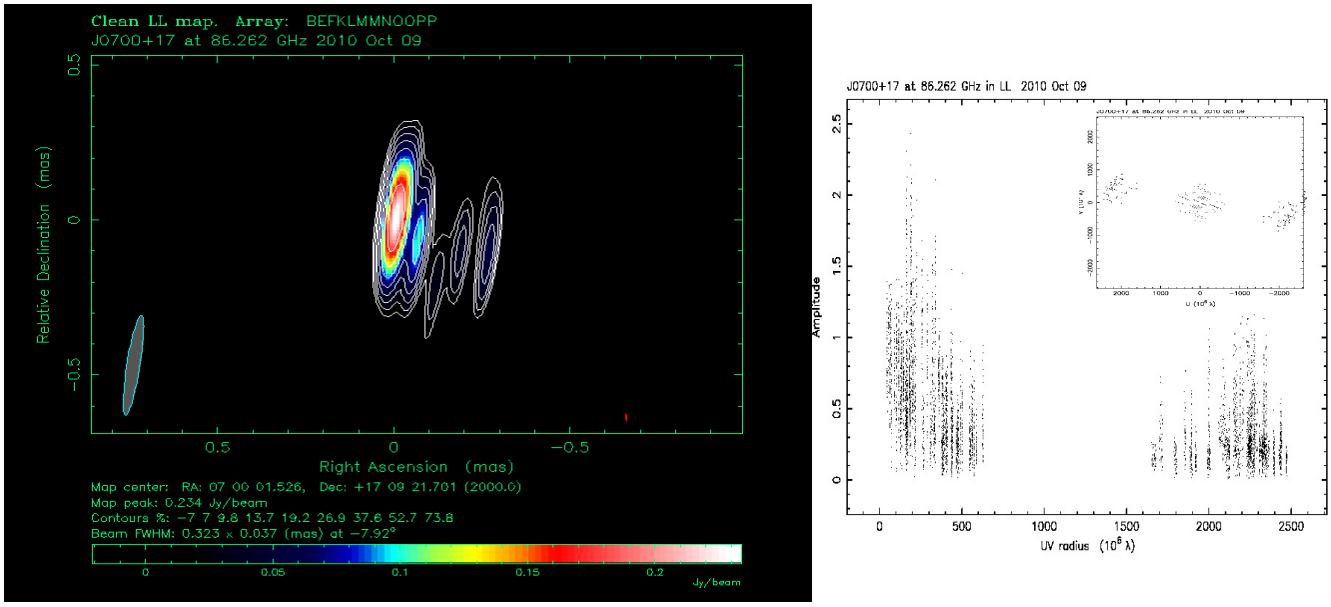

Fig.2. *3mm map of J0956+2515(Oct 2010). Image is convolved with the natural beam The contour lines start at 3 times the rms noise level. The lowest contour is at 7 mJy. Negative contours are shown with dashed gray lines (on the left). The visibility amplitude vs UV radius is shown on the right panel with uv coverage in the inset on the right panel.*

b. J1130+3815

The source is a quasar at redshift of 1.766. In the image in the Fig.2a, we identify one feature in the jet extending along P.A 180degree at a distance of 0.1256 mas.The peak flux density is 0.278 Jy/beam,with a beam size of 0.1961x0.04171 mas and the lowest contour is at 9 mJy. The brightness temperature of the core component is1.545x10^{11} K.

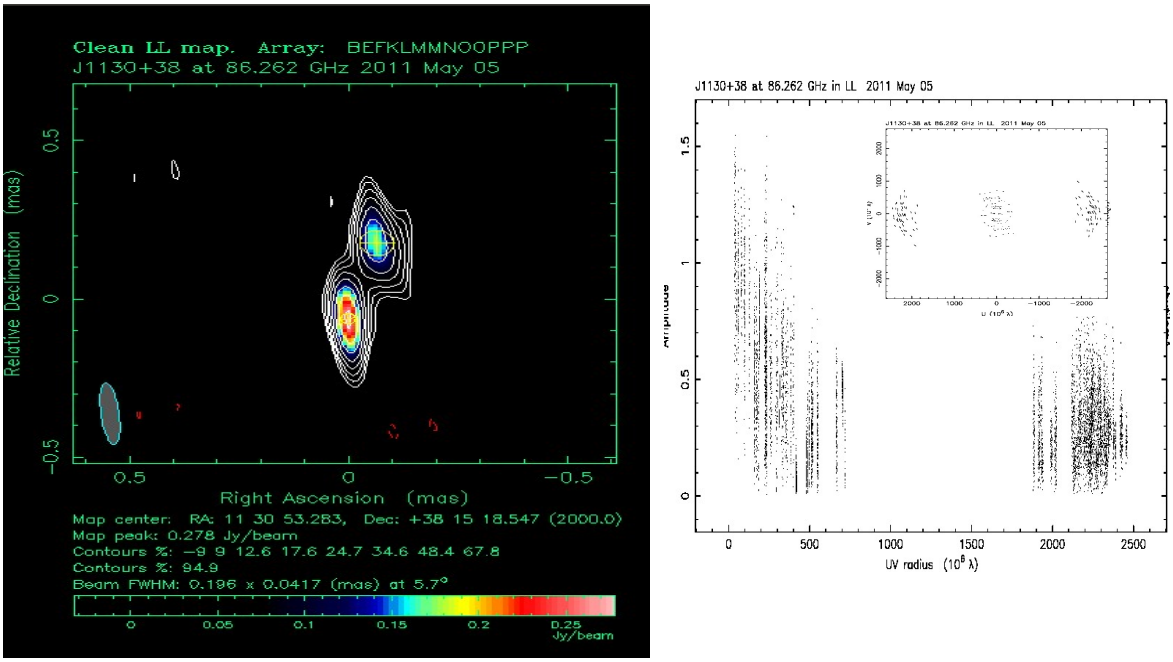

Fig.2a. *3mm map of J1130+3815(May 2011). Image is convolved with the natural beam.The contour lines start at 3 times the rms noise level. The lowest contour is at 9 mJy. Negative contours are shown with dashed gray lines (on the left). The visibility amplitude vs UV radius is shown on the right panel with uv coverage in the inset on the right panel.*

We also present the images of two bright calibrator sources 3C345 and 0716+714. The images presented for the calibrators is made from just one or two scans of 4 minutes each. Despite the fact that this survey is done in a snapshot mode of 4-5 scans of just 7-8 minutes with poor uv coverage, the maps and flux density of the calibrators are in good agreement with the well established 3mm maps of the same sources and this shows the general qualityof the survey data and the 3mm maps of weak target sources.

c. 3C345

The source is an optically violent variable quasar at a redshift of 0.595. In the image in the Fig.3, we identify three jet components .These components can be identified with similar orientation of the jet in the VLBI image at 43 GHz and at 15 GHz. The peak flux density is 0.463 Jy/beam , with a beam size of 0.242x0.0343 mas and the lowest contour is at 12 mJy. The brightness temperature of the core component is 1.053×10^{11}k.

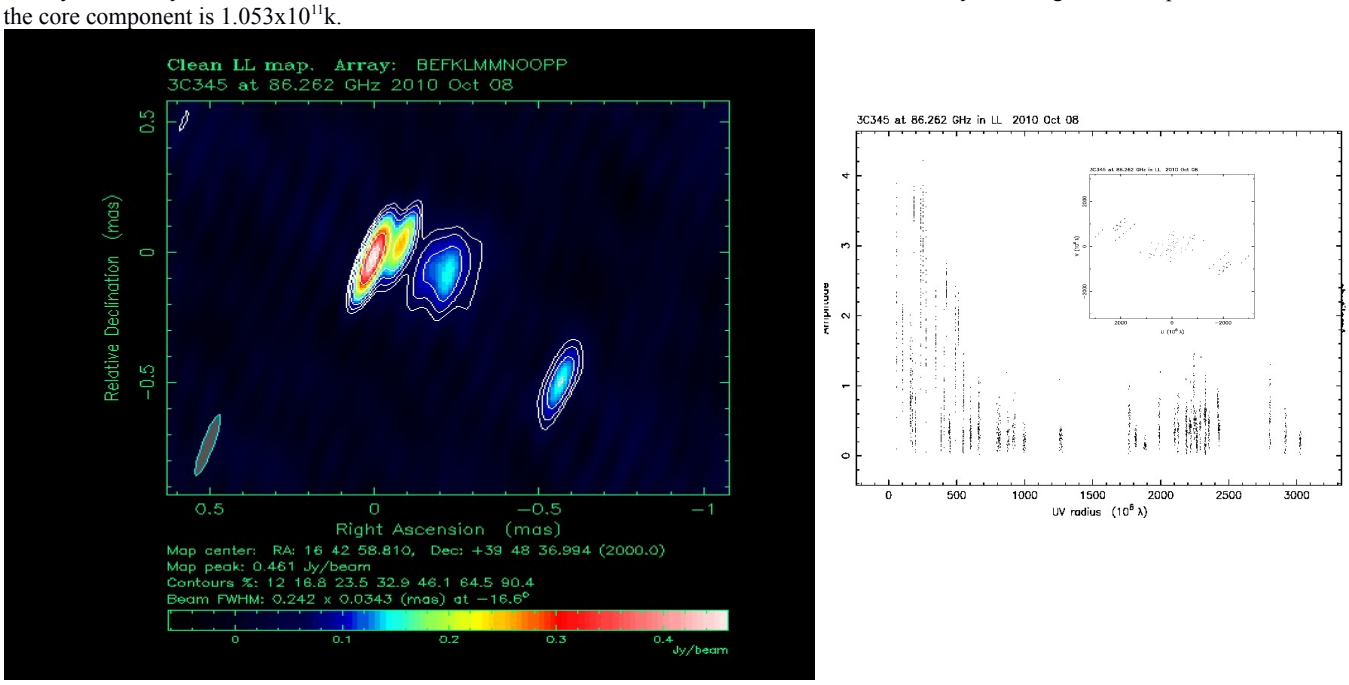

Fig.3. *3mm map of 3C345 (Oct 2010). Image is convolved with the natural beam.The contour lines start at 3 times the rms noise level. The lowest contour is at 12 mJy. Negative contours are shown with dashed gray lines (on the left). The visibility amplitude vs UV radius is shown on the right panel with uv coverage in the inset on the right panel.*

d. 0716+714

The source is a BL Lac object at a redshift ≥ 0.3. In the image in the Fig.3a, we identify 3 jet components.These components can be identified with similar orientation of the jet in the VLBI image at 43 GHz and at 15 GHz. The peak flux density is 4.2 Jy/beam , with a beam size of 0.05523x0.03961 mas and the lowest contour is at 6.2 mJy. The total flux density of the source after the modelfitting with circular gaussian components is 3.01813 mJy.The brightness temperature of the core component is 9.711×10^{11} k.

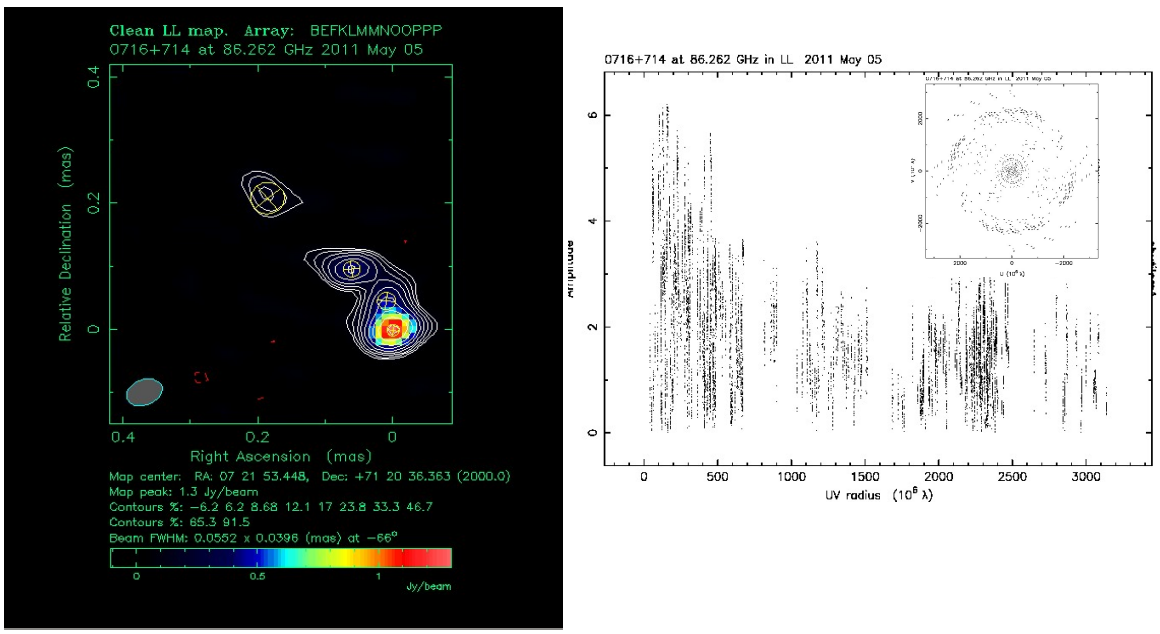

Fig.3a. *3mm map of 0716+714 (May 2011). Image is convolved with the natural beam.The contour lines start at 3 times the rms noise level. The lowest contour is at 6.2 mJy. Negative contours are shown with dashed gray lines (on the left). The visibility amplitude vs UV radius is shown on the right panel with uv coverage in the inset on the right panel.*

The hybrid maps and modelfit paramets for the physical properties of all the 168 compact radio sources will be presented in detail Nair.D.G., *PhDthesis,in prep.*

3.2 *Brightness temperature and Jet physics*

Using the gaussian model fitting on the cleaned images, we have paramaterized the total flux density,S_t, the post fit rms, σ_{rms}, size,d, distance,r and position angle,θ, to the jet components from which we measured the brightness temperature of the VLBI cores and jets.The brightness temperature (T_b) of the emission region which is modelled by a gaussian component with the total flux density S_{tot} and the angular size d (=) θ_{FWHM} is given by

$$T_b = 1.22 \times 10^{12} \frac{S_{tot}(1+z)}{(d^2 \upsilon^2)} \quad \text{------- (1)}$$

expressed in kelvin, where λ is the wavelength, z is the redshift and k_B is the Boltzman constant. The factor (1+z) reflects the cosmological effect on the observed brightness temperature. For the sources with unknown redshift, we calculated the brightness temperature simply in the observer's frame of reference. The minimum resolvable size of the component was also taken into account while calculating the brightness temperature. The minimum resolvable limit,d_{min} of a gaussian component is given in Lobanov 2005as

$$d_{min} = \left\{ \frac{2^{(1+\beta)/2}}{\pi} \right\} \left\{ \pi ab \ln 2 \ln \frac{(SNR+1)}{(SNR)} \right\}^{(1/2)} \quad \text{------- (2)}$$

where a and b are the axes of the restoring beam, SNR is the signal to noise ratio, β is the weighing function which is 0 for natural weighting or 2 for uniform weighting. So if the size of the gausssian component,d is less than d_{min}, then the brightness temperature is obtained with $d = d_{min}$ which is the lower limit on T_b. The brightness temperature measured in our VLBI images can be used to study the general properties of compact jets.

3.2.1 *Distribution of brightness temperature in the VLBI core and jet components*

Fig.4 shows the distibution of the population of T_b in the VLBI core and jet components and Fig.5 shows the distribution of the measured brightness temperature in the source frame frequency plane.The mean and median of the distribution of T_b is 1.776×10^{11} K and 8.349×10^{10} K for the VLBI cores and the mean and median of the T_b distribution is 2.254×10^{10} K and 9.158×10^{9} K for the inner jet components (r < 1pc). Fig.4 suggests that there may be a difference between the distribution of brightness temperature measured in the cores (red) and jets (cyan).There is a difference in the average Tb distribution measured in the cores and inner jet components by a factor of 7.88.

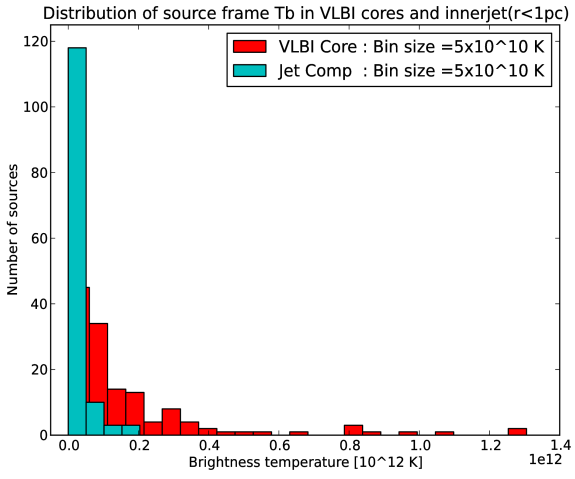

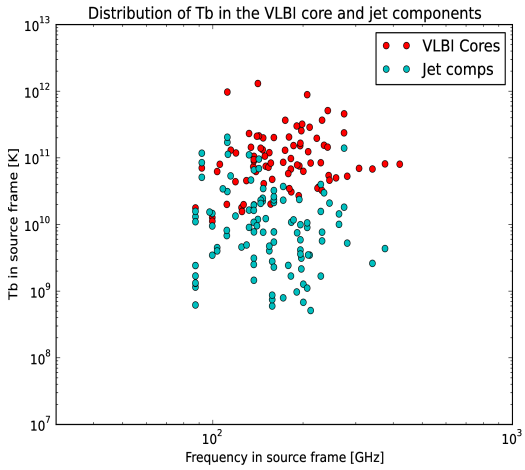

Fig.4 .*Distribution of the source frame brightness temperatures in the cores and jet components* Fig.5. *Distribution of observed T_b in the source frame frequency plane.*

It is interesting that the T_b distribution in concentrated within $T_b < 4 \times 10^{11}$ kelvin for VLBI cores(within the first 8 bins) and within $T_b < 5.0 \times 10^{10}$ kelvin for inner jet components (within the first bin). So the T_b of VLBI cores are in certain agreement with the inverse compton limit (~ 5×10^{11} K, Kellermann & Pauliny-Toth 1969) and T_b of jet components are also in agreement with the equipartition

limit (~ $5x10^{10}$ K,Readhead 1994) which has to verified with further modelling.

3.2.2 *Testing the adiabatic expansion of jets*

Assuming that each of the jet components is an independent relativistic shock with adiabatic energy losses dominating the emission (Marsher 1990,Lobanov 2000 and Lee 2008).The jet plasma has a power law distribution $N(E)dE \alpha E^{-s}$ dE and the magnetic field falls down as $B \alpha d^{-a}$,where d is the transverse dimension in the jet. By these assumptions, we can relate the brightness temperatures $T_{b,J}$ of the jet components to the brightness temperature $T_{b,C}$ of the core as :

$$T_{b,J} = T_{b,C} (d_J/d_C)^{\xi} \text{ ---------(3)}$$

where d_J and d_C are the measured sizes of jet component and core respectively and $\xi = [2(2s+1)+3a(s+1)]/6$.

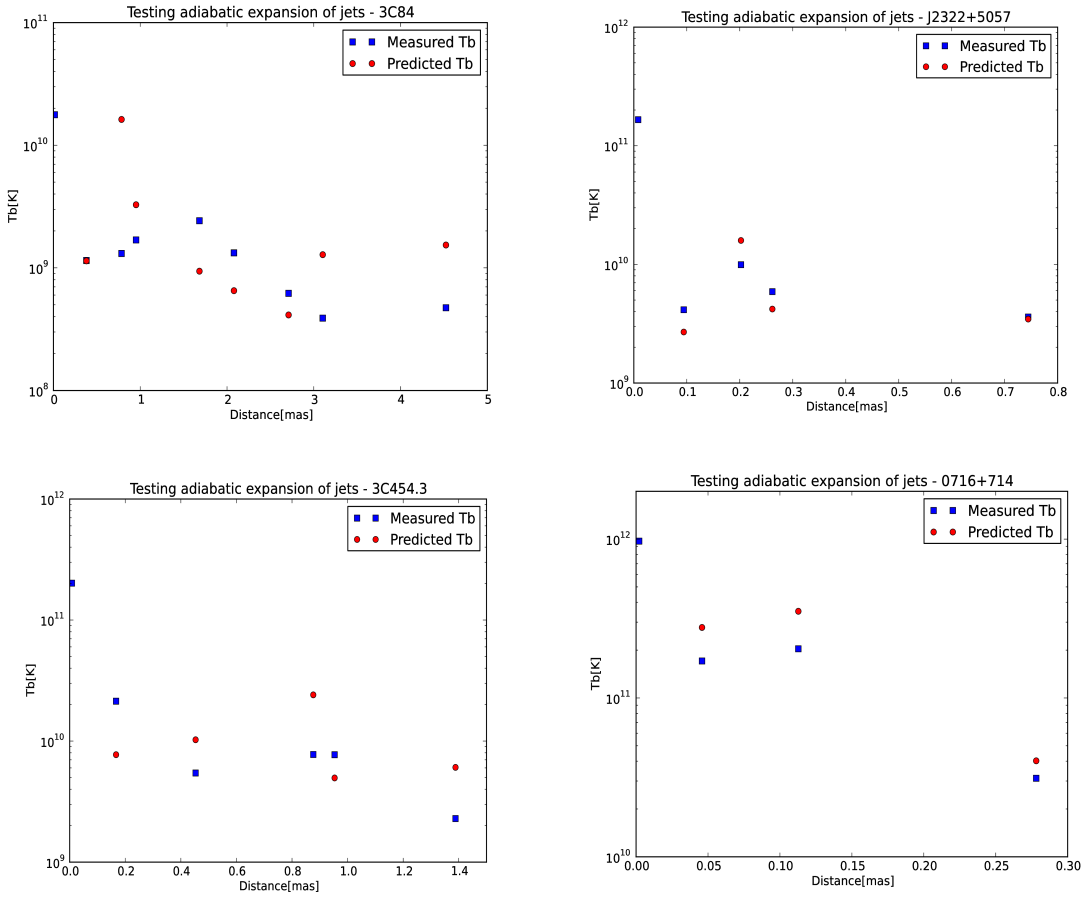

Fig.6. *Changees of the brightness temperature along the jet of four sources – 3C84, J2322-5037, 3C454.3 and 0716+714 from this survey. Blue squares and red circles represent the measured Tb from this survey and theoretically predicted Tb if the jets expand adiabatically. The initial brightness temperature in each jet is assumed to be same as that measured in the VLBI core.*

According to synchrotron emission with spectral index $\alpha = -0.5$ we have taken energy spectral index $s = 2.0$ and $a = 1$ for the transverse structure of the magnetic field in the jet. For sources with sufficient structural detail detected in our survey, we have investigated the effect of adiabatic energy losses on the evolution of brightness temperature along the jet. Fig.6 shows this testing of adiabatic expansion and changes of the brightness temperature along the jets in several sources.
The measured and predicted values of Tb agrees well ,irrespective of the assumptions on spectral index, magnetic field etc. This strongly suggests that the jet components will be plane shocks which expand adiabatically.

3.3 *Brightness temperature measurement from another method – directly from the interferometric visibility data*

Other than the imaging and model fitting method applied to determine the image parameters ie., flux density and angular size and thereby determine the brightness temperature by modelling the structure of the emitting region ($T_{b,mod}$) ,we have also applied another completely independent method to measure the upper limits on brightness temperature ($T_{b,lim}$) as Lobanov 2015. We compare the brightness temperatures obtained from the model fits with estimates of the brightness temperature limits made directly from the visibility data.This method is successfully tested in low frequencies for eg. in 15 GHz MOJAVE (Kovalev 2005) complete sample in Lobanov 2015. Since this method doesnot apply any imaging of the source structure from a uv coverage,it is independent of whether

the uv coverage is robust or not. The interferometric visibility is expressed as $V = V_q e^{-i\phi_q}$ described by its amplitude V_q and phase ϕ_q. The angular extent, θ, of the emitting region can be determined from V_q as

$$\theta = \frac{2\sqrt{ln2}\,\lambda\sqrt{\ln\frac{V_q+\sigma_q}{V_q}}}{(\pi B)} \quad \text{------- (4)}$$

where σ_q is the error in visibility amplitude and B is the baseline distance. From the angular extent, we have calculated T_b by simply applying Rayleigh- Jeans limit to Planck's formula and thus T_b is formulated as

$$T_{b,limit} = \frac{\pi B^2}{2k}(V_q+\sigma_q)\left(\ln\frac{V_q+\sigma_q}{V_q}\right)^{-1} \quad \text{------- (5)}$$

For each object, the $T_{b,lim}$ is estimated from the 86 GHz data at uv radius ≥ 0.9 Bmax using (5), where B_{max} is the maximum baseline distance, inorder to restrict the visibility information to the most compact structures. The limiting $T_{b,lim}$ are essentially equal to $T_{b,mod}$ estimated from imaging method which is shown in Fig.7. We can see a clear one to one correspondance between the two and this verifies the fidelity of T_b measurements.

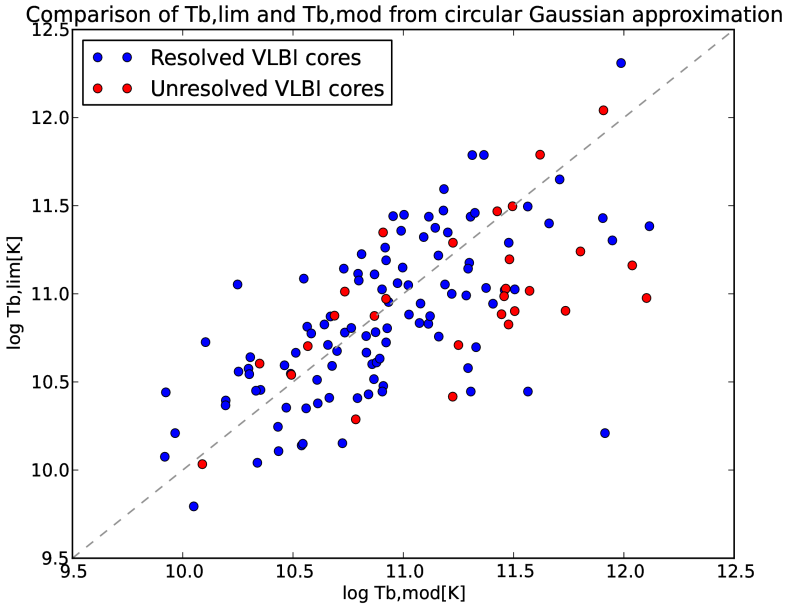

Fig.7. *The one to one correspondance of T_b measured from circular gaussian approximation of source structure from the 3mm maps and T_b estimated from the theoretical calculation from the direct interferometric visibilities.*

3.4 *Tb measurements in high frequency Vs low frequency*

The brightness temperature of the VLBI cores from this 86 GHz survey with similar estimates from the MOJAVE VLBI surveys at 15 GHz is presented in Fig.8.

Indeed, a compilation of brightness temperatures measured at 15 and 86 GHz indicates that the brightness temperatures measured at 86 GHz are systematically lower by an average factor of ~ 10 (Fig.8). Previous studies by Lobanov 2000 suggest that the value of υ_{break}, below which energy losses begin to dominate emission is below 86 GHz and Lee 2008 suggests that υ_{break} can be as low as 20 GHz. So if T_o starts to decrease as seen in Fig.8 at 86GHz, there will be only a few sources suitable for VLBI at 147 GHz, 215 GHz and higher frequencies. Such a decrease of T_o will also provide a strong argument in favour of the decelerating jet model or particle cascade models as discussed by Marscher1995. This supports the theoretical model that the relativistic electron-positron pair plasma up-scatter the photons produced outside the jet into X-rays and γ rays. This will basically decelerate the jet and decreases the Lorentz factor along the jet. We can see a hint of corelation between the observed brightness temperature and apparent Jet speed taken from MOJAVE survey(Kovalev 2005) in Fig.9.

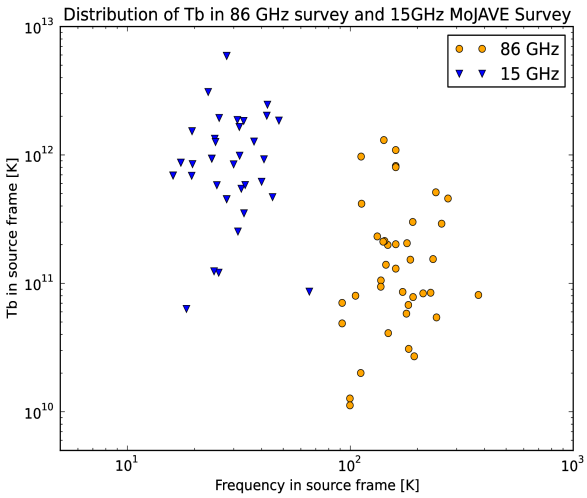

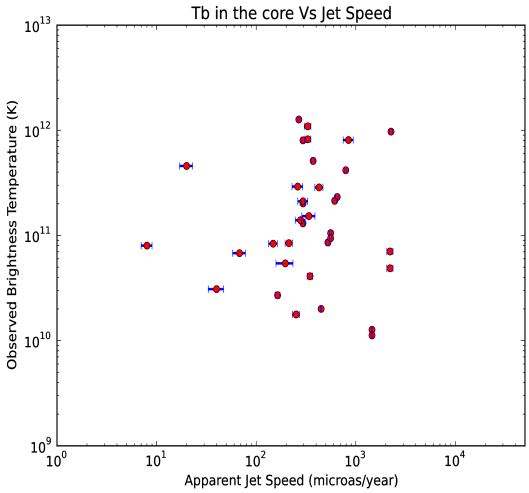

Fig.8. *The comparison of T_b distribution at 15 GHz and 86 GHz in the frequency plane* Fig.9.*Measured Tb at 86 GHz Vs apparent jet speed taken from 15 GHz MOJAVE survey.*

We will further compile the T_b measurements from other 1.6 GHz, 2.3 GHz ,8.4 GHz ,5 GHz ,22 GHz and 43 GHz low frequency surveys with the 86 GHz T_b measurements.This comparison with different frequencies can be used to constrain the bulk Lorentz factor and the intrinsic brightness temperature,T_o of the jet plasma, using different types of population models of relativistic jets (Vermeulen & Cohen 1994, Homan et al. 2006). This procedure will yield excellent measures of the $T_0(\upsilon)$ and $T_o(r)$ evolution in jets, which will enable distinguishing between the acceleration and deceleration scenario for the flow as discussed in Marscher 1995 and testing several alternative acceleration scenarios of the relativistic jets including the radiation pressure (Bodo 1985), tangled magnetic field (e.g., Heinz & Begelman 2000), and MHD acceleration (Vlahakis & Königl 2004) models.

References

Beasley, A.J.,Dhawan,V., Doeleman,S., & Philips,R.B. 1997, in Millimeter-VLBI Science Workshop,ed. R.Barvainis & R.B. Philips, 53

Bodo,G.,1985, A&A, 149,246

Cohen,M.H., Lister,M.L.,Homan,D.C., et al. 2007, ApJ, 658, 232

Cornwell,T.J & Fomalont,E., 1999,in Synthesis Imaging in Radio Astronomy II,ed G.B Taylor,C.L.Carilli, & R.A. Perley, 187- 199

Heinz,S. & Begelman,M.C., 2000, ApJ, 535, 104

Homan,D.C., Kovalev,Y.Y., Lister,M.L., et al. 2006, ApJ, 642, L115

Kellermann,K.I., & Pauliny -Toth,I.I., 1969, ApJ, 155, L71

Kovalev,Y.Y., Kellermann,K.I., Lister,M.L., et al. 2005, AJ, 130, 2473

Lee,S.S., 2007, PhD thesis, University of Bonn

Lee,S.S., Lobanov,A.P., Krichbaum,T.P., et al. 2008, AJ, 136, 159

Lister,M.L & Homan,D.C.,2005,AJ, 130,1389

Lobanov,A.P.,1996,PhD thesis, New Mexico Institute of Mining and Technology, Socorro, USA

Lobanov,A.P., Krichbaum,T.P., Graham,D.A., et al. 2000, A&A, 364, 391

Lobanov,A., 2015, A&A, 574, A84

Lonsdale,C,J., Doelman,S.S., & Philips,R.B 1998, AJ, 116, 8

Marsher,A.P. 1995, Proceedings of the national Academy of Science, 92, 11439

Nair,D.G., *86 GHz VLBI Survey of Ultracompact Radio Emission in Active Galactic Nuclei,*PhD Thesis at University of Köln,in prep.

Petrov,L., et al. 2007, AJ, 133, 2487

Rantakyro,F.T., Baath,L.B., Backer,D.C., et al. 1998, A&AS, 131, 451

Readhead,A.C.S., 1994, ApJ, 426, 51

Shepherd,M.C., Pearson,T.J., & Taylor,G.B., 1994,BAAS,26,987

Vermeulen,R.C & Cohen,M.H., 1994, ApJ, 430, 467

Vlahakis,N. & Königl,A. 2004, ApJ, 605, 656